IOPscience iopscience.iop.org

Home Search Collections Journals About Contact us My IOPscience

Retarded modes in layered magnetic structures containing left-handed materials

This article has been downloaded from IOPscience. Please scroll down to see the full text article.

2008 J. Phys.: Condens. Matter 20 335210

(http://iopscience.iop.org/0953-8984/20/33/335210)

View the table of contents for this issue, or go to the journal homepage for more

Download details:
IP Address: 129.252.86.83
The article was downloaded on 29/05/2010 at 13:54

Please note that terms and conditions apply.

J. Phys.: Condens. Matter **20** (2008) 335210 (5pp) doi:10.1088/0953-8984/20/33/335210

Retarded modes in layered magnetic structures containing left-handed materials

Na Liu, Xiao-Dong Hou and Xiangdong Zhang

Department of Physics, Beijing Normal University, Beijing 100875, People's Republic of China

Received 3 June 2008
Published 22 July 2008
Online at stacks.iop.org/JPhysCM/20/335210

Abstract

We present a theoretical study of magnetic excitations in ferromagnetic film embedded in the left-handed materials (LHMs) and in superlattices composed of alternating layers of ferromagnetic materials and the LHMs. The dispersion relations of the surface polaritons in these systems are solved exactly. Some unusual retarded modes are found in these systems in comparison with the conventional ferromagnetic–dielectric multilayer structures. Magnetic excitations in the long-wavelength limit have also been discussed, and unusual magnetostatic modes have also been obtained.

1. Introduction

During the past decades ultrathin films and multilayers of ferromagnetic materials have been the subject of intensive studies [1, 2]. Some physical properties in these structures such as giant magnetoresistance and collective magnetic excitations have proved most interesting and unique, which cannot be found in bulk magnetic matter. Surface magnon modes for the case of a ferromagnetic slab under the nonmagnetic dielectric background were first investigated by Damon and Eshbach in the magnetostatic approximation [3]. The corresponding surface and bulk propagation wave dispersions for alternating magnetic–nonmagnetic multilayer structures were calculated by Camley *et al* [4, 5]. Without the use of the magnetostatic approximation, the retarded modes in the ferromagnetic slab and ferromagnetic–nonmagnetic superlattices had also been discussed by Karsono *et al* [6] and Barnas [7], respectively. Subsequently, further discussions on such a subject in semi-infinite magnetic–nonmagnetic superlattices and other structures had been done by many authors [8–15]. Since the understanding of the excitation spectrum of surface and bulk waves within these structures is essential in predicting the performances of devices incorporating layer structures, these investigations are important and necessary.

However, the above investigations all focus on ferromagnetic and dielectric systems. Recently, left-handed materials (LHMs) have attracted a great deal of attention from both theoretical and experimental sides [16–19]. These materials, which are characterized by simultaneous negative permittivity and permeability, possess a number of unusual electromagnetic effects [16–19]. One of them is that negative refraction can occur at the interface between the LHMs and a positive (conventional) medium [20, 21]. The other is that some new surface polarized modes around a left-handed slab can appear [22]. In addition, a one-dimensional stack of layers with alternating positive and negative refraction materials with zero averaged refractive index displays an unusual transmission bandgap [23] and some unique properties of the beam transmission [24].

It is natural to ask what kind of phenomenon will occur when we combine the ferromagnetic slab with the LHMs? Can the new excitation modes appear for layered magnetic structures containing LHMs in comparison with conventional magnetic–nonmagnetic multilayer dielectric structures? If some new excitation modes can be found, it is of particular interest for microwave and optical signal processing such as optical communications and waveguides for magnetostatic modes. Considering these problems, in this paper we calculate the retarded wave spectrum of magnetic layered systems composed of alternating ferromagnetic and left-handed material (LHM) layers based on the technique developed in [25, 6, 7]. The excitation modes in the magnetostatic limit will also be discussed.

2. Magnetic excitations of ferromagnetic films immersed in the LHM

We first consider a single ferromagnetic slab with thickness d immersed in the LHM background. The y axis of a

 © 2008 IOP Publishing Ltd Printed in the UK

Cartesian coordinate system is taken normal to the film, whose boundaries are taken as $y = -d/2$ and $d/2$. The magnetization M_S in the ferromagnetic slab is parallel to the film surfaces and parallel to the z direction. The film is supposed to have infinite extent in the z and x directions. The magnetic field $\vec{H}$ in the ferromagnetic slab satisfies the following Maxwell equation:

$$\nabla^2\vec{H} - \nabla(\nabla\cdot\vec{H}) - \frac{\varepsilon\overleftrightarrow{\mu}}{c^2}\frac{\partial^2\vec{H}}{\partial t^2} = 0, \tag{1}$$

where c is the light velocity in the vacuum and magnetic permeability tensor is written as

$$\overleftrightarrow{\mu} = \begin{pmatrix} \mu_{xx} & \mu_{xy} & 0 \\ -\mu_{xy} & \mu_{xx} & 0 \\ 0 & 0 & \mu_{zz} \end{pmatrix}, \tag{2}$$

where

$$\mu_{xx}(\omega) = \mu\left(1 + \frac{\omega_m\omega_0}{\omega_0^2 - \omega^2}\right), \tag{3}$$

$$\mu_{xy}(\omega) = \mathrm{i}\mu\left(\frac{\omega_m\omega}{\omega_0^2 - \omega^2}\right), \tag{4}$$

with $\omega_0 = \gamma H_0$, $\omega_m = 4\pi\gamma M_0$ and $M_0 = \frac{M_s}{\mu}$. Here M_0 is the static magnetization, H_0 is the static field, γ is the gyromagnetic ratio and μ is the high frequency permeability.

In the LHMs, the Maxwell equation is written as

$$\nabla^2\vec{H} - \frac{\varepsilon(\omega)\mu(\omega)}{c^2}\frac{\partial^2\vec{H}}{\partial t^2} = 0, \tag{5}$$

where

$$\varepsilon(\omega) = 1.0 - \frac{\omega_{\mathrm{p}}^2}{\omega^2}, \qquad \mu(\omega) = 1.0 - \frac{F\omega^2}{\omega^2 - \omega_{l0}^2}. \tag{6}$$

Here ω_{p} is the plasma frequency and ω_{l0} is the magnetic resonance frequency. The solutions for three regions in the Voigt geometry can be expressed as

$$\vec{H}_T = \vec{T}_{x,y}\exp(-\alpha y)\exp\mathrm{i}(kx - \omega t) \qquad y > \frac{d}{2} \tag{7}$$

$$\vec{H}_T = [\vec{F}_{x,y}\exp(\beta y) + \vec{G}_{x,y}\exp(-\beta y)]\exp(\mathrm{i}(kx - \omega t)) \qquad -\frac{d}{2} < y < \frac{d}{2} \tag{8}$$

$$\vec{H}_T = \vec{R}_{x,y}\exp(\alpha y)\exp\mathrm{i}(kx - \omega t) \qquad y < -\frac{d}{2}, \tag{9}$$

where

$$\alpha^2 = k^2 - \frac{\omega^2}{c^2}\varepsilon(\omega)\mu(\omega) \tag{10}$$

and

$$\beta^2 = k^2 - \mu_v\frac{\omega^2}{c^2} \tag{11}$$

with $\mu_v = \mu_{xx} + \frac{\mu_{xy}^2}{\mu_{xx}}$.

According to the condition $\nabla\cdot(H + M) = 0$, the coefficients $\vec{T}_{x,y}$, $\vec{F}_{x,y}$, $\vec{G}_{x,y}$ and $\vec{R}_{x,y}$ satisfy the following relations:

$$\frac{T_x}{T_y} = \frac{\alpha}{\mathrm{i}k} \qquad \frac{R_x}{R_y} = -\frac{\alpha}{\mathrm{i}k} \tag{12}$$

$$\frac{F_x}{F_y} = -\frac{\mathrm{i}k\mu_{xy} + \beta\mu_{xx}}{\mathrm{i}k\mu_{xx} - \beta\mu_{xy}} \qquad \frac{G_x}{G_y} = -\frac{\mathrm{i}k\mu_{xy} - \beta\mu_{xx}}{\mathrm{i}k\mu_{xx} + \beta\mu_{xy}}. \tag{13}$$

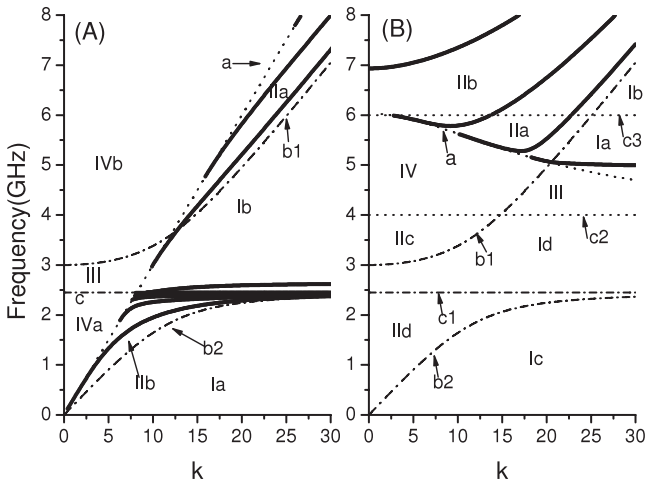

Figure 1. Dispersion relations for a ferromagnetic film immersed in the dielectric background (A) and the LHM background (B). Here $\omega_0 = 2.0$ GHz, $\omega_m = 1.0$ GHz, $\mu = 1.75$ and $d\omega_0/c = 0.3$. The different regions in the k–ω plane are marked. I (a, b, c, d) correspond to real α and real β; II (a, b, c, d) to real α and imaginary β; III to imaginary α and real β; IV to imaginary α and imaginary β. The dashed–dotted lines b1 and b2 denote the dispersion curves of bulk magnon polaritons in the ferromagnetic system. The dotted lines c2, c3, a and c1 correspond to $\omega = 4.0$ GHz, $\omega = 6.0$ GHz, $k = \sqrt{\varepsilon(\omega)\mu(\omega)}\omega/c$ and $\omega_v = \sqrt{\omega_0(\omega_0 + \omega_m)}$, respectively. Solid lines represent the modes obtained by equation (14). $\varepsilon(\omega) = \mu(\omega) = 1$ is taken in the dielectric background.

Applying the boundary conditions of continuity for the tangential component of magnetic field and magnetization, we can obtain the following equation:

$$\left[\alpha^2\mu_v^2 + \mu^2(\omega)\left(k^2\frac{\mu_{xy}^2}{\mu_{xx}^2} + \beta^2\right)\right] \times \tanh(\beta d) + 2\alpha\beta\mu_v\mu(\omega) = 0. \tag{14}$$

The retarded modes can be obtained by solving equation (14). They depend on α and β through equations (10) and (11), respectively. According to the values of α and β, in general one can distinguish the following four situations [9–14]:

(i) α and β are both real. The wave is localized at the interfaces, where the amplitude of the wave varies exponentially when one moves from any interface into the magnetic or LHM layer.

(ii) α is real and β is imaginary. The wave is exponentially localized at surfaces in the LHM films and is oscillatory (extended) in the magnetic layers.

(iii) α is imaginary and β is real. The wave is exponentially localized in the magnetic film and extended in the LHM layers.

(iv) α and β are both imaginary. The corresponding wave is extended in both magnetic and LHMs.

The k–ω plane can be divided into different regions corresponding to the above four situations. These regions are cut apart by some curves, which are shown in figure 1(B). The dashed–dotted lines b1 and b2 denote the dispersion curves of bulk magnon polaritons in the ferromagnetic system

(Voigt configuration), which correspond to $k^2 = \frac{\omega^2}{c^2}\mu_v$. The dotted line c1 is defined as $\omega_v = \sqrt{\omega_0(\omega_0+\omega_m)}$. The dotted curve *a* represents $k = \sqrt{\varepsilon(\omega)\mu(\omega)}\omega/c$, which is similar to the photon line in the air. Here $\omega_0 = 2.0$ GHz, $\omega_m = 1.0$ GHz, $\mu = 1.75$ and $d\omega_0/c = 0.3$ are taken in the ferromagnetic slab [12–15]. We take $\omega_p = 10$ GHz, $\omega_{l0} = 4.0$ GHz and $F = 0.56$ in the LHMs. The material is left-handed (negative n) between $\omega = 4.0$ and 6.0 GHz [22, 17]. Here the dotted lines c2 and c3 correspond to $\omega = 4.0$ GHz and 6.0 GHz, respectively.

Solid lines in figure 1(B) represent the solutions of equation (14). Here the discussion is focused on the negative n region. Two modes are found in the Ia region, which result from the interaction between the surfaces waves of separate magnetic layers. Similarly, two modes are obtained in the IIa region, which represent the guided magnetic polaritons of the ferromagnetic slab. All modes converge to $k = \sqrt{\varepsilon(\omega)\mu(\omega)}\omega/c$. For cases (iii) and (iv) (imaginary α), the solutions of equation (14) represent extended modes in the LHMs or whole systems. Due to the semi-infinite stack of the LHMs for the present system, the separate modes do not exist in (iii) and (iv) situations.

In order to compare the present results with the previous investigations on the retarded modes of the ferromagnetic slab in the dielectric background, in figure 1(A) we display the calculated results from equation (14) when $\varepsilon(\omega) = \mu(\omega) = 1$. Here the dashed–dotted lines and dotted lines represent a similar meaning to those in figure 1(B). Solid lines also represent the resolutions of equation (14) for $\varepsilon(\omega) = \mu(\omega) = 1$. Our results agree with those in [12, 13]. Comparing the results in figure 1(A) with those in figure 1(B), we find that the regions in the k–ω plane not only change, both the number and the changing trend of the retarded modes are also different between them.

These differences originate from the different surface polaritons in the ferromagnetic–LHM structure. In the previous investigations, new surface polaritons have been found around the LHM slab, cylinder and sphere in comparison with the corresponding dielectric systems [22]. The present results show that the different surface polaritons also exist in the ferromagnetic–LHM structure in comparison with those of conventional ferromagnetic–dielectric structures. Such a feature can be seen more clearly in the long-wavelength limit (magnetostatic approximation). Taking the magnetostatic approximation ($\frac{\omega}{c} \to 0$) for equation (14), we can obtain the equation of magnetostatic modes as

$$\omega^2 = \omega_0^2 + \omega_0\omega_m + \frac{\omega_0\omega_m[\mu^2-\mu^2(\omega)]+\mu^2\omega_m^2}{\mu^2(\omega)-2\mu(\omega)\coth(q_\parallel L)+\mu}. \quad (15)$$

If $\mu(\omega)$ is taken as 1.0, equation (15) is reduced to known results of magnetostatic modes for a ferromagnetic slab in the dielectric background, which had been analyzed in [3, 8]. Figures 2(a) and (b) present the comparison between two kinds of case. It is shown that only one mode (figure 2(a)) can be found for the conventional ferromagnetic–dielectric structure and two modes appear for the ferromagnetic–LHM system. The above discussions only focus on one kind of thickness of the ferromagnetic slab. In fact, if we take various thicknesses of the slab, similar phenomena can be obtained. Such features can also be found in the ferromagnetic–LHM superlattices.

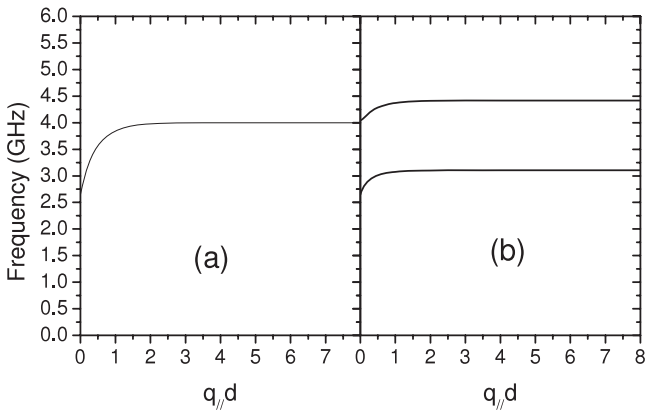

Figure 2. The frequency magnetostatic modes as a function of $q_\parallel d$. (a) Ferromagnetic slab immersed in the dielectric background; (b) ferromagnetic slab immersed in the LHM background. Here $q_Z = 0$, $\omega_0 = 1.0$ and $\omega_m = 6.0$.

3. Magnetic excitations in ferromagnetic–LHM superlattices

Now let us consider a ferromagnetic superlattice composed of alternating ferromagnetic films of thickness d_1 and LHM films of thickness d_2. In each magnetic film the magnetization M_S (and applied magnetic field) is parallel to the film surface and parallel to the z direction. The layers are supposed to have infinite extent in the z and y directions. One may write the fields in the form $H \sim \exp[\mathrm{i}(k_y y + k_z z)]$, where k_y and k_z are the components of the two-dimensional wavevector $k_\parallel$. Here we consider only the case of $k_z = 0$ and write k_y simply as k. Thus, the magnetic field in the ferromagnetic layer can be written as

$$\vec{H}(\vec{r};t) = \vec{H}(x,k;\omega)\,\mathrm{e}^{\mathrm{i}(ky-\omega t)}, \qquad nL < x < nL + d_1. \quad (16)$$

We only consider the case when the magnetic field of the wave is perpendicular to the axis of spontaneous magnetization. So, one may assume $H_z(y,k;\omega) = 0$. The remaining components of the amplitude $H(x,k;\omega)$ can be written as

$$H_i(x,k;\omega) = B_i^+(n)\,\mathrm{e}^{\beta x'} + B_i^-(n)\,\mathrm{e}^{-\beta x'}; \qquad i = x, y \quad (17)$$

for $0 < x' = x - (n-1)L < d_1$. The coefficients $B^+_{x(y)}(n)$ and $B^-_{x(y)}(n)$ are determined by $\nabla\cdot(\vec{h}+\vec{m}) = 0$. They satisfy the following relations:

$$\frac{B_x^\sigma(n)}{B_y^\sigma(n)} = \mathrm{i}\frac{(\omega^2/c^2)\mu_x(\omega)-\sigma k\beta}{k^2-(\omega^2/c^2)\mu_\perp(\omega)}; \qquad \sigma = +, -, \quad (18)$$

where σ on the right-hand side is understood as $\sigma f = f$ for $\sigma = +$ and $\sigma f = -f$ for $\sigma = -$. In contrast, the magnetic field in the LHM films can be written as

$$\vec{H}(x,k;\omega) = A^+(n)\,\mathrm{e}^{\alpha x'} + A^-(n)\,\mathrm{e}^{-\alpha x'} \quad (19)$$

for $d_1 < x' = x - (n-1)L < L$. The coefficients $A_x^\sigma(n)$ and $A_y^\sigma(n)(\sigma = +, -)$ satisfy the following relationship:

$$A_x^\sigma(n) = -\mathrm{i}\frac{\sigma k}{\alpha} A_y^\sigma(n). \tag{20}$$

Applying the boundary continuity conditions for the tangential component of $\vec{H}$ and the normal component of $\vec{H} + \vec{M}_s$, the following relations can be obtained:

$$\begin{pmatrix} A_y^+(n) \\ A_y^-(n) \end{pmatrix} = \vec{R} \begin{pmatrix} B_y^+(n) \\ B_y^-(n) \end{pmatrix} \tag{21}$$

and

$$\begin{pmatrix} B_y^+(n+1) \\ B_y^-(n+1) \end{pmatrix} = \vec{S} \begin{pmatrix} A_y^+(n) \\ A_y^-(n) \end{pmatrix}, \tag{22}$$

where the elements of the 2×2 matrices $\vec{R}$ and $\vec{S}$ are given by the expressions

$$R_{11(22)} = \frac{1}{2}\left[1 + \frac{\alpha}{\mu(\omega)} \frac{\beta\mu_\perp \mp k\mu_x}{k^2 - \frac{\omega^2}{c^2}\mu_\perp}\right] \mathrm{e}^{\pm(\beta-\alpha)d_1}, \tag{23}$$

$$R_{12(21)} = \frac{1}{2}\left[1 - \frac{\alpha}{\mu(\omega)} \frac{\beta\mu_\perp \pm k\mu_x}{k^2 - \frac{\omega^2}{c^2}\mu_\perp}\right] \mathrm{e}^{\mp(\beta-\alpha)d_1}, \tag{24}$$

$$S_{11(22)} = \frac{\alpha\beta\mu_\perp \pm \alpha k\mu_x + (k^2 - \frac{\omega^2}{c^2}\mu_\perp)\mu(\omega)}{2\alpha\beta\mu_\perp} \mathrm{e}^{\pm\alpha L}, \tag{25}$$

$$S_{12(21)} = \frac{\alpha\beta\mu_\perp \pm \alpha k\mu_x - (k^2 - \frac{\omega^2}{c^2}\mu_\perp)\mu(\omega)}{2\alpha\beta\mu_\perp} \mathrm{e}^{\mp\alpha L} \tag{26}$$

in which the upper sign refers to the indices in the parentheses. Equations (21) and (22) combine to give

$$\begin{pmatrix} B_y^+(n+1) \\ B_y^-(n+1) \end{pmatrix} = \vec{T} \begin{pmatrix} B_y^+(n) \\ B_y^-(n) \end{pmatrix}, \tag{27}$$

where $\vec{T} = \vec{S}\vec{R}$, which has the property $\det \vec{T} = 1$. Applying Bloch's theorem, we can also obtain

$$\begin{pmatrix} B_y^+(n+1) \\ B_y^-(n+1) \end{pmatrix} = \mathrm{e}^{\mathrm{i}q_z L} \begin{pmatrix} B_y^+(n) \\ B_y^-(n) \end{pmatrix}, \tag{28}$$

where q_z is the component of the wavevector, $-\pi/L < q_z \leqslant \pi/L$. From equations (27) and (28), we can obtain the following equation:

$$\cos(q_z L) = \cosh(\beta d_1)\cosh(\alpha d_2) + \left[\frac{\mu(\omega)(k^2 - \frac{\omega^2}{c^2}\mu_\perp)}{2\alpha\beta\mu_\perp} + \frac{\alpha}{2\beta\mu(\omega)}\mu_v(\omega)\right]\sinh(\beta d_1)\sinh(\alpha d_2). \tag{29}$$

This is just the general dispersion equation for a wave propagating perpendicularly to the magnetization in the superlattice consisting of alternating ferromagnetic films and LHMs. If $\varepsilon = 1$ and $\mu = 1$ are taken, equation (29) gives the results of a conventional ferromagnetic–dielectric superlattice [14]. From equation (29), the dispersion curves for two kinds of case can be easily obtained by numerical calculations.

The calculated results (solid lines) of the dispersion relation for two kinds of case are plotted in figures 3(A) and (B), respectively. The dotted lines and dashed–dotted lines are identical with those in figures 1(A) and (B). For the ferromagnetic–dielectric superlattice, our results in figure 3(A) are also in agreement with the previous investigations in [14]. Comparing them with those in figure 3(B), we find that dramatic differences appear. Some differences in the IIa and Ia regions between figures 3(A) and (B) are similar to those between figures 1(A) and (B) for the single ferromagnetic slab. The unique part for the case of the superlattice in comparison with that of a single ferromagnetic slab can exhibit in the III region (imaginary α and real β). In the III region, no solution can be found for the case of a single ferromagnetic slab, which has been analyzed in section 2. In contrast, there are many solutions in this region for the ferromagnetic–LHM superlattice. This means that many guide modes can exist in the LHM layer of the ferromagnetic–LHM superlattice. This is also in obvious contrast to the ferromagnetic–dielectric superlattice, where only one mode is found in the III region of figure 3(A). Such a difference is also due to the unusual excitation properties in the LHMs or on the interface of the ferromagnetic–LHM structure.

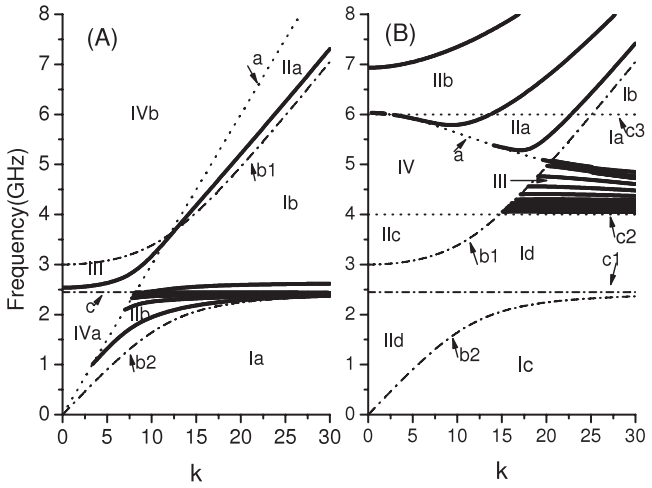

Figure 3. Dispersion relations for a ferromagnetic superlattice. (A) corresponds to the superlattice composed of alternating ferromagnetic films of thickness d_1 and dielectric films of thickness d_2; (B) corresponds to that composed of alternating ferromagnetic films of thickness d_1 and LHM films of thickness d_2. Here $\omega_0 = 2.0$ GHz, $\omega_m = 1.0$ GHz, $\mu = 1.75$ and $d\omega_0/c = 0.3$ ($d_1 = d_2 = d$). The different regions in the k–ω plane are marked. I (a, b, c, d) correspond to real α and real β; II (a, b, c, d) to real α and imaginary β; III to imaginary α and real β; IV to imaginary α and imaginary β. The dashed–dotted lines b1 and b2 denote the dispersion curves of bulk magnon polaritons in the ferromagnetic system. The dotted lines c2, c3, a and c1 correspond to $\omega = 4.0$ GHz, $\omega = 6.0$ GHz, $k = \sqrt{\varepsilon(\omega)\mu(\omega)}\omega/c$ and $\omega_v = \sqrt{\omega_0(\omega_0 + \omega_m)}$, respectively. Solid lines represent the modes obtained by equation (15). $\varepsilon(\omega) = \mu(\omega) = 1$ is taken in the dielectric background.

In the magnetostatic approximation ($\frac{\omega}{c} \to 0$), the magnetostatic equation for the superlattice can also be obtained similar to the case of a single ferromagnetic slab:

$$\omega^2 = \frac{2\mu(\omega)\cdot\mu\cdot\omega_0(\omega_0+\omega_m) + \Delta\cdot[\mu(\omega)^2\omega_0^2 + (\omega_0+\omega_m)^2]}{2\mu(\omega)\cdot\mu + \Delta\cdot[\mu^2 + \mu(\omega)^2]}, \tag{30}$$

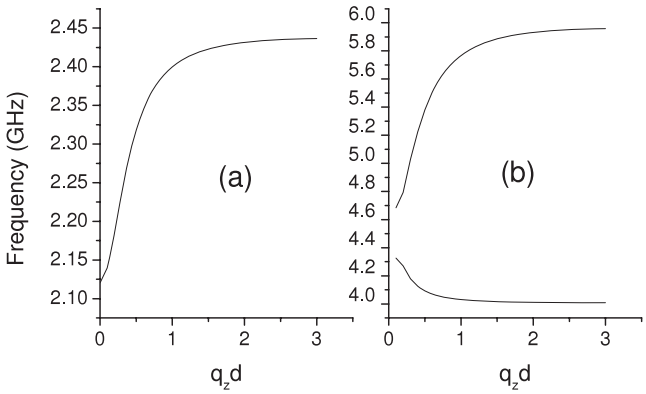

Figure 4. The frequency of magnetostatic modes as a function of $q_Z L$. (a) Ferromagnetic superlattice composed of alternating ferromagnetic films of thickness d_1 and dielectric films of thickness d_2; (b) ferromagnetic superlattice composed of alternating ferromagnetic films of thickness d_1 and LHM films of thickness d_2. Here $d_1 = d_2 = d$ and $q_\parallel d = 0.2$. The other parameters are identical with those in figure 3.

where

$$\Delta(q_\parallel, q_z) = \frac{\sinh(q_\parallel d_1)\sinh(q_\parallel d_2)}{\cosh(q_\parallel d_1)\cosh(q_\parallel d_2) - \cos(q_z L)}. \qquad (31)$$

This is also identical with the previous results in [4–8] when $\mu(\omega) = 1$ is taken for equation (30). If $\mu(\omega)$ and $\varepsilon(\omega)$ are given by equation (6), new magnetostatic modes can appear. Figure 4 shows such a character. Figure 4(b) corresponds to the superlattice with the ferromagnetic and LHM materials, while (a) corresponds to that with the ferromagnetic and dielectric materials. Two curves in figure 4(b) and one curve in figure 4(a) are observed again, which is similar to the case of a single ferromagnetic slab in section 2.

4. Summary

We have calculated the magnetic excitations in the ferromagnetic film embedded in the LHMs and in the superlattices composed of alternating layers of ferromagnetic materials and the LHMs. The dispersion relations in these systems are solved exactly. New surface polaritons are not only found in the present system in comparison with those of conventional ferromagnetic–dielectric structures, the changing trends of the modes as a function of wavevector are also demonstrated to be different between them. These differences are not only for the retarded modes, they are also for the magnetostatic modes in the long-wavelength limit. From previous investigations, we know that the interaction between the excitation modes can be exploited for devices such as microwave spectrum analyzers, optical frequency shifters, tunable optical filters and optical beam deflectors [2]. With the findings of these new excitation modes, we anticipate that the functions of these devices can be improved by using the ferromagnetic–LHM system instead of the conventional ferromagnetic–dielectric structure. That is to say, our present results can provide important references in designing microwave and optical signal devices.

Acknowledgments

This work was supported by the National Natural Science Foundation of China (grant no. 10674017) and the National Key Basic Research Special Foundation of China under grant 2004CB719804.

References

[1] Heinrich B 1994 *Ultrathin Magnetic Structures* ed B Heinrich and J A C Bland (Heidelberg: Springer)
[2] Cottam M G and Tilley D R 1989 *Introduction to Surface and Superlattice Excitation* (Cambridge: Cambridge University Press)
[3] Damon R W and Eshbach J R 1961 *J. Phys. Chem. Solids* **19** 308
[4] Camley R E, Rahman T S and Mills D L 1983 *Phys. Rev.* B **27** 261
[5] Grunberg P and Mika K 1983 *Phys. Rev.* B **27** 2955
[6] Karsono A D and Tilley D R 1978 *J. Phys. C: Solid State Phys.* **11** 3487
[7] Barnas J 1987 *Solid State Commun.* **61** 405
[8] Camley R E and Cottam M G 1987 *Phys. Rev.* B **35** 189
[9] Barnas J 1988 *J. Phys. C: Solid State Phys.* **21** 1021
Barnas J 1988 *J. Phys. C: Solid State Phys.* **21** 4097
[10] Villeret M, Rodriguez S and Kartheuser E 1989 *Phys. Rev.* B **39** 2583
[11] Raj N and Tilley D R 1987 *Phys. Rev.* B **36** 7003
[12] Wang X Z and Tilley D R 1994 *Phys. Rev.* B **50** 13472
[13] Polushkin N I, Michalski S A, Yue L and Kirby R D 2006 *Phys. Rev. Lett.* **97** 256401
[14] Marchand M and Caille A 1980 *Solid State Commun.* **34** 827
[15] How H and Vittoria C 1989 *Phys. Rev.* B **39** 6823
How H and Vittoria C 1989 *Phys. Rev.* B **39** 6831
[16] Veselago V G 1968 *Sov. Phys.—Usp.* **10** 509
[17] Smith D R, Padilla W J, Vier D C, Nemat-Nasser S C and Schultz S 2000 *Phys. Rev. Lett.* **84** 4184
Shelby R A, Smith D R and Schultz S 2001 *Science* **292** 77
[18] Pendry J B 2000 *Phys. Rev. Lett.* **85** 3966
[19] Agranovich V M and Gartstein Y N 2006 *Phys.—Usp.* **49** 1029
Agranovich V M and Gartstein Y N 2007 *Physics of Negative Refraction and Negative Index Materials* ed C M Krowne and Y Zhang (Berlin: Springer)
[20] Ziolkowski R W and Heyman E 2001 *Phys. Rev.* E **64** 056625
[21] Wu L, He S L and Shen L F 2003 *Phys. Rev.* B **67** 235103
[22] Ruppin R 2001 *J. Phys.: Condens. Matter* **13** 1811
Ruppin R 2000 *Phys. Lett.* A **277** 61
Ruppin R 2004 *J. Phys.: Condens. Matter* **16** 5991
[23] Li J, Zhou L, Chan C T and Sheng P 2003 *Phys. Rev. Lett.* **90** 083901
[24] Shadrivov I V, Sukhorukov A A and Kivshar Y S 2003 *Appl. Phys. Lett.* **82** 3820
[25] Economou E N 1969 *Phys. Rev.* **182** 539